Ferroelectric domain walls in PbTiO$_3$ are effective regulators of heat flow at room temperature

Eric Langenberg*[,1,2], Dipanjan Saha[3], Megan E. Holtz[1,4], Jian-Jun Wang[5], David Bugallo[2], Elias Ferreiro-Vila[2], Hanjong Paik[1], Isabelle Hanke[6], Steffen Ganschow[6], David A. Muller[4], Long-Qing Chen[5], Gustau Catalan[7], Neus Domingo[7], Jonathan Malen[3], Darrell G. Schlom*[,1,8], Francisco Rivadulla*[,2]

[1]Department of Materials Science and Engineering, Cornell University, Ithaca, New York 14853, USA.

[2]CiQUS-Universidade de Santiago de Compostela, Santiago de Compostela 15782, Spain

[3]Mechanical Engineering Department, Carnegie Mellon University, Pittsburgh, Pennsylvania 15213, USA.

[4]School of Applied and Engineering Physics, Cornell University, Ithaca, New York 14853, USA.

[5]Department of Materials Science and Engineering, Pennsylvania State University, State College, Pennsylvania 16802, USA.

[6]Leibniz-Institut für Kristallzüchtung, Max-Born-Straße 2, 12489 Berlin, Germany

[7]Catalan Institute of Nanoscience and Nanotechnology (ICN2), CSIC, Barcelona Institute of Science and Technology, Campus Universitat Autònoma de Barcelona, Bellaterra, 08193 Barcelona, Spain.

[8]Kavli Institute at Cornell for Nanoscale Science, Ithaca, New York 14853, USA.

ABSTRACT. Achieving efficient spatial modulation of phonon transmission is an essential step on the path to phononic circuits using "phonon currents." With their intrinsic and reconfigurable interfaces—domain walls (DWs)—ferroelectrics are alluring candidates to be harnessed as dynamic heat modulators. This paper reports the thermal conductivity of single-crystal $PbTiO_3$ thin films over a wide variety of epitaxial-strain-engineered ferroelectric domain configurations. The phonon transport is proved to be strongly affected by the density and type of DWs, achieving a 61% reduction of the room-temperature thermal conductivity compared to the single-domain scenario. The thermal resistance across the ferroelectric DWs is obtained, revealing a very high value ($\approx 5.0 \times 10^{-9}$ Km^2W^{-1})—comparable to grain boundaries in oxides—, explaining the strong modulation of the thermal conductivity in $PbTiO_3$. This low thermal conductance of the DWs is ascribed to the structural mismatch and polarization gradient found between the different types of domains in the $PbTiO_3$ films, resulting in a structural inhomogeneity that extends several unit cells around the DWs. These findings demonstrate the potential of ferroelectric DWs as efficient regulators of heat flow in one single material—overcoming the complexity of multilayers systems and the uncontrolled distribution of grain boundaries—, paving the way for applications in phononics.

Classical strategies to control the propagation of phonons are based on the design of artificial interfaces, i.e. grain boundaries[1] or interfaces in multilayer heterostructures[2,3]. Indeed, this approach has been widely used for reducing the thermal conductivity, κ, in thermoelectric devices[1,4]. Unfortunately, the arrangement of these interfaces is fixed once the material is fabricated, which eliminates the possibility of dynamically tuning phonon transport. In this regard, ferroelectric DWs can be as effective as multilayer interfaces and grain boundaries in inhibiting the transmission of phonons[5–7], but with the added advantage of being reconfigurable. Recent phonon-transport calculations in multidomain $PbTiO_3$ predict a strong suppression in the transmission of transverse phonons across DWs, leading to a $\approx$30-50% calculated decrease of κ [8,9]. A reduction of κ with the density of DWs has been experimentally observed at low temperatures in bulk single crystals of $BaTiO_3$, KH_2PO_4 and LiF[5–7] and more recently at room temperature in multiferroic $BiFeO_3$ by Hopkins *et al.*,[10] although these results were challenged by Ning *et al.*[11] In addition, the experiments performed by Mante and Volger[5] proved that a large increase in κ can be achieved by the application of an electric field, which reduces the DW density, yet the effect is only significant at temperatures below 30 K. Ihlefeld *et al.*[12] achieved $\approx$11-13% electric-field-induced reduction of κ at room temperature in polycrystalline $Pb(Zr_{0.3}Ti_{0.7})O_3$ films. In contrast, suspended membranes of the same composition show $\approx$13% increase of κ when an electric field is applied.[13] The presence of grain boundaries in polycrystalline $Pb(Zr_{0.3}Ti_{0.7})O_3$ films results in a lack of homogeneity throughout the sample in terms of domain configurations—each individual grain possesses different distributions of DWs—leading to a random and nonuniform modulation of the phonon transport across the film. This severely reduces the effectiveness of the electric field-modulation of κ when compared to theoretical values and makes it difficult to disentangle the role played by DWs from grain boundaries and vacancies. First-principles calculations revealed that κ

in single-domain PbTiO$_3$ can vary (10-20%) by applying an electric field,[14] similar to what is found in polycrystalline Pb(Zr$_{0.3}$Ti$_{0.7}$)O$_3$ films,[12,13] but in this case the variation is caused by the structural response (phonon-phonon scattering) without the need of changing the DW distribution.
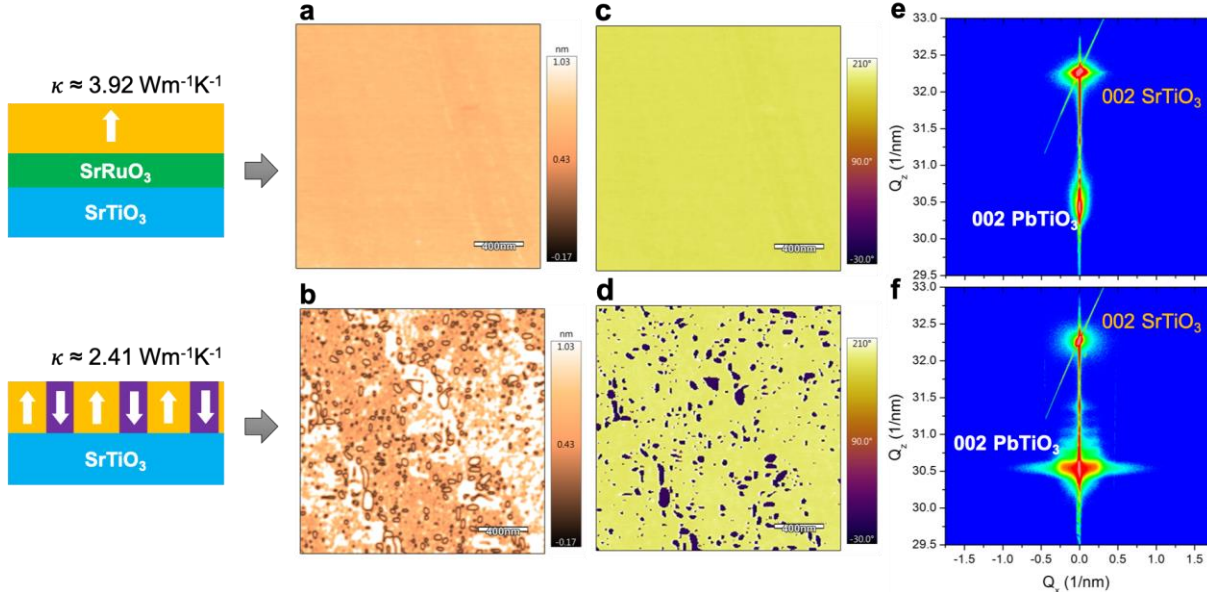

Figure 1. Single-domain vs. high density of 180° DWs in PbTiO$_3$/SrRuO$_3$/SrTiO$_3$ and PbTiO$_3$/SrTiO$_3$, respectively. Left panels depict the single *c*-domain (upper panel) and the *c*-(up/down) multidomain (lower panel), together with the corresponding thermal conductivity values measured by FDTR. PFM vertical amplitude images of PbTiO$_3$ deposited on SrRuO$_3$-buffered SrTiO$_3$ substrate (a), and of PbTiO$_3$ deposited directly on a substrate of SrTiO$_3$ (b). The corresponding PFM phase images of these samples for PbTiO$_3$/SrRuO$_3$/SrTiO$_3$ (c) and for PbTiO$_3$/SrTiO$_3$ (d). X-ray RSM around the 002 Bragg reflection of PbTiO$_3$ for the heterostructure PbTiO$_3$/SrRuO$_3$/SrTiO$_3$ heterostructure (e), and for PbTiO$_3$/SrTiO$_3$ (f).

To clarify this situation it is of paramount importance to experimentally determine the intrinsic thermal resistance of ferroelectric DWs at room temperature and disentangle it from other potential contributions, in order to evaluate the suitability and performance of ferroelectrics in the emerging field of phononics.[15–17] For this purpose, we have grown single-crystal PbTiO$_3$ thin films (thickness = 50 nm) by reactive molecular-beam epitaxy (MBE) on several substrates with different lattice constants to induce a wide variety of homogenous ferroelectric domain patterns in PbTiO$_3$ through epitaxial strain engineering.[18–21] The growth details are found in the Supp. Info.

4

Using this strategy, we demonstrate that κ can be strongly reduced by engineering different ferroelectric DW configurations and we identify what DW patterns are most effective at achieving this reduction.

To create a single-domain reference sample free of ferroelectric DWs, we deposit an epitaxial single crystal thin-film of $PbTiO_3$ on a (001) $SrTiO_3$ substrate (strain = -1.36%) with a 10 nm thick buffer layer of conducting $SrRuO_3$.[22] During the same deposition, $PbTiO_3$ is also deposited directly onto a neighboring bare $SrTiO_3$ substrate without the conducting layer. In Figure 1a-d we show the vertical piezoresponse force microscopy (PFM) images of the two $PbTiO_3$ films, revealing that in both cases the polarization is exclusively out-of-plane (see Supp. Info.). The absence of the conducting layer results in ubiquitous 180° ferroelectric DWs separating c-domains with the polarization up and down (Figure 1b,d), in contrast to the single-domain scenario when $PbTiO_3$ is deposited on a conducting layer (Figure 1a,c). The change in the c-domain pattern is further corroborated by X-ray reciprocal space maps (RSM) around the 002 Bragg reflection (Figure 1 e,f). The single c-domain scenario gives rise to a sharp XRD peak around the 002 reflection of $PbTiO_3$, whereas the mixture of c-up and c-down domains produces a substantial in-plane broadening of this peak. The thermal conductivity of both films was measured by frequency-domain thermoreflectance (FDTR)[23,24] (see Supp. Info). Note that, due to the small thickness of the films and the geometry of the FDTR measurements (see Supp. Info), the thermal conductivity obtained is mainly the cross-plane component with minor contribution of in-plane components. This is extended to all the thermal conductivity measurements in this work.

The results obtained for single-domain $PbTiO_3$, $\kappa \approx 3.9 \pm 0.2$ W m^{-1}K^{-1} is very similar to the prediction by first-principles calculations.[14,25] In contrast, the nucleation of ferroelectric 180° DWs causes a substantial suppression of the room-temperature κ by $\approx$39%: $\kappa \approx 2.4 \pm 0.1$ W m^{-1}K^{-1} for

the *c*-(up/down) multidomain structure. This remarkable reduction indicates that 180° DWs play a significant role in modulating the phonon transport—despite the fact that, structurally, the domains they separate are identical.
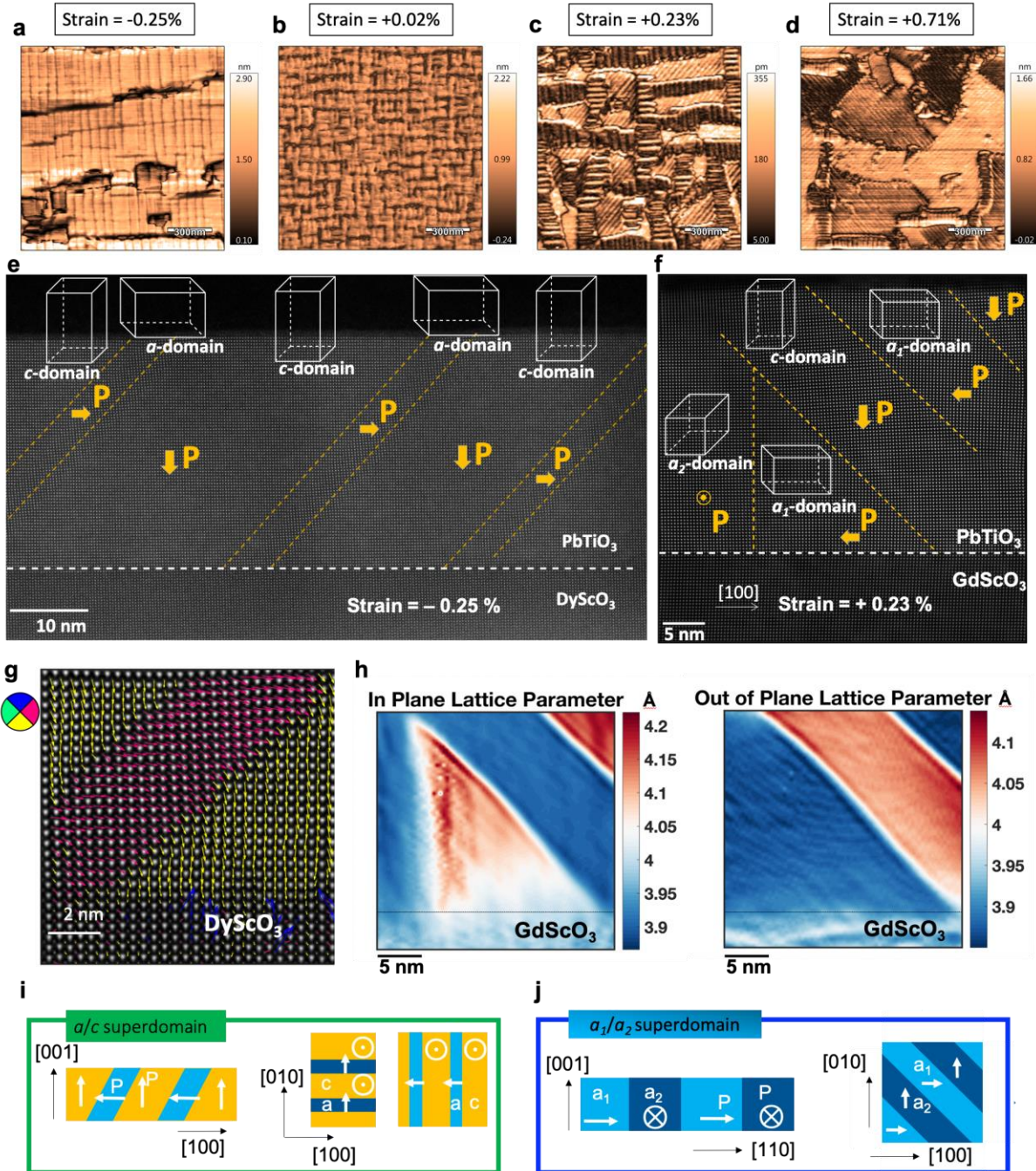

Figure 2. Introduction of various types of 90° DW patterns by strain engineering in PbTiO₃ thin films. Vertical PFM amplitude images of PbTiO₃/SrRuO₃ films deposited on DyScO₃ (a) and TbScO₃ (b) substrates. Lateral PFM amplitude images of PbTiO₃/SrRuO₃ films on GdScO₃ (c) and

SmScO$_3$ (d) substrates. The PFM images are aligned with the [010] (horizontal axis) and [100] (vertical axis) pseudocubic directions. Cross-sectional STEM images of PbTiO$_3$ on DyScO$_3$ (e), showing the a/c domain architecture, and of PbTiO$_3$ on GdScO$_3$ (f), showing the coexistence of a/c and a_1/a_2 superdomains. g) Atomic-scale polarization maps of PbTiO$_3$ on DyScO$_3$ from the Ti displacements in the STEM image in (e). h) In-plane and out-of-plane lattice parameter obtained from the atomic-resolution STEM image in (f) using the substrate for reference. Sketch describing the a/c (i) and the a_1/a_2 (j) domain patterns.

In order to account for the intrinsic thin film thermal conductivity, the contribution from the interface thermal resistance, R$_{Int}$, must be accurately determined. For that purpose, we measure the thermal conductivity for three different thicknesses of PbTiO$_3$ on SrTiO$_3$ with a constant 10 nm thick buffer layer of SrRuO$_3$ in between (see methods and Fig. S4 of the supporting information). In this configuration the films of PbTiO$_3$ are single-domain, so an accurate estimation of the interface resistance of the samples can be made. We have used this R$_{Int}$ for the rest of the samples used in this work. The additional interface between SrRuO$_3$ and SrTiO$_3$ is not present in the other samples, so this should be the largest possible R$_{int}$. A possible overestimation of R$_{Int}$ implies an overestimation of k_{film} (see Equation S1), so that the actual thermal conductivity reduction by domain wall scattering may be even larger than reported in this conservative approach.

Also, given that the area probed by the laser beam ($\approx$114 μm^2) is much larger than the domain size ($\approx$20-60 nm) (see Figure 1), both ferroelectric domains with polarization up and down, as well as domain walls, are simultaneously probed in each experiment. This is applicable for all the sample measured in this work (see the discussion of Figure 2 below).

Next, we assess the effect of 90° DWs. PbTiO$_3$ was epitaxially grown on different rare-earth scandate substrates to progressively modify the biaxial strain from compressive towards tensile, and therefore to gradually change the density and type of DWs (see Supp. Info.). The amplitude PFM images for each epitaxial strain value (Figure 2a-d) depict the large variety of DW

configurations achieved by strain engineering. The coexistence of different domains is further observed by cross-sectional scanning transmission electron microscopy STEM (Figure 2e-h), where a_1 and a_2-, and c-domains signals the polarization lying along [100], [010] and [001] pseudocubic directions, respectively (see Supp. Info.). In contrast to PbTiO$_3$ on SrTiO$_3$ (Figure 1) where 180° DWs are present, the DWs here (Figure 2) are 90° ferroelectric-ferroelastic DWs. The evolution of the domain structures with strain follows a clear trend: for low compression a/c domain architecture (sketch depicted in Figure 2i) is stabilized, in which the a/c DW density increases on approaching the ≈0% strain; crossing into the tensile strain side the nucleation of a-domains is even further promoted, gradually dominating the domain configuration and, thus, producing a progressively increase of the a_1/a_2 superdomains (sketch depicted in Figure 2j). Further details about the strain-dependence of the ferroelectric domain patterns in PbTiO$_3$ are found in the Supp. Info. In short, strain engineering allows us to modify, at will, the ferroelectric domain structures in PbTiO$_3$: pure c-domains, a/c domain patterns—with different DW density— and targeted ratios of a/c and a_1/a_2 90° DWs. This offers a unique opportunity to probe the effect of the different types of ferroelectric DWs on the propagation of phonons.

Figure 3a shows κ of the PbTiO$_3$ films as a function of strain, along with the DW periodicity (the mean ferroelectric domain size) obtained from analyzing the PFM images (see Figure S9 in Supp. Info.). The results show a significant modulation of κ, around 34%, and an excellent correlation with the DW periodicity: the smaller the DW periodicity (≡larger DW density), the lower the κ. For the sake of comparison, the previously measured κ of the single-domain scenario and the c-up/c-down pattern (180° DWs) are also indicated in Figure 3a. As observed, a much stronger suppression of κ is found upon introduction of a-domains in tensile-strained PbTiO$_3$ thin films, reaching the remarkable value of 61% reduction with regard to the single-domain scenario, the

largest reduction at room temperature ever reported in ferroelectrics. Although epitaxial strain also changes the ratio between *a* and *c*-domains, its effect on the thermal conductivity does not seem to be significant (see Figure S10 and Supp. Info.).
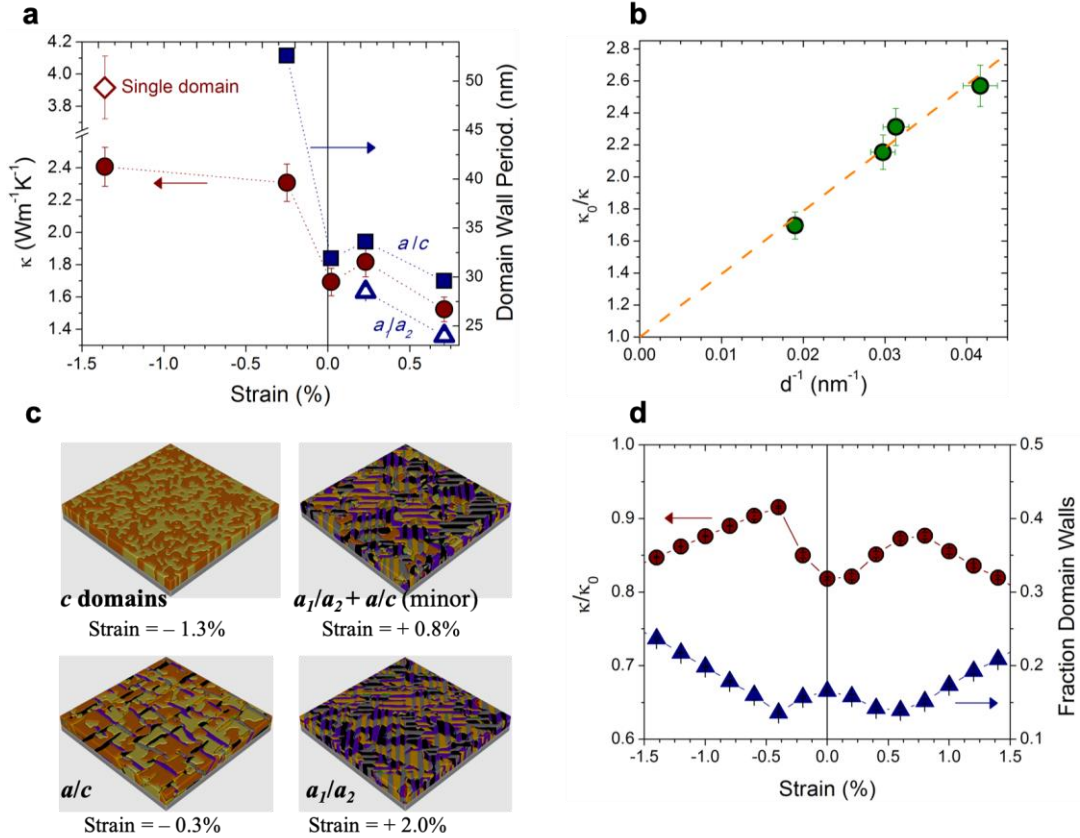

Figure 3. Effect of ferroelectric DWs on the thermal conductivity of PbTiO$_3$ at room temperature. a) Room-temperature thermal conductivity and DW periodicity (obtained from PFM analysis) of PbTiO$_3$ as a function of epitaxial strain. b) Fitting of the thermal conductivity to the Kaptiza resistance model (linearized Equation (1), see text). κ_0 stands for the thermal conductivity of the single-domain. c) Strain-dependent domain patterns obtained from phase-field simulations. The fraction of *a*-domains increases progressively with respect to c-domains, as tensile strain increases. d) Strain-dependent thermal conductivity (normalized by κ_0) and fraction of domain walls with regard to domains of PbTiO$_3$ predicted by the phase-field simulations [see Experimental Section].

The strong reduction of κ observed suggests that DWs are very effective phonon-scatterers, probably over a wide range of wavelengths.[9] The predicted thermal conductivity accumulation

function shows that $\approx$70% of the room temperature κ of PbTiO$_3$ comes from phonons having a mean free path less than 10 nm.[25] Given that the domain sizes—measured by PFM and TEM—are larger, the reduced κ cannot result from reductions in the mean free path alone, and DW boundaries must hence offer a Kapitza thermal resistance, R_{DW}. Our ferroelectric films can thus be considered as homogeneous domains of length d and thermal conductivity k_0, separated by regularly spaced DWs with R_{DW}. The temperature drop across the sample is divided between the interior of the domain and at the DW, which, using the model derived by Nan and Birringer,[26] results in a reduction of the thermal conductivity as follows:

$$\frac{\kappa_0}{\kappa} = 1 + \frac{2\kappa_0 R_{DW}}{d} \qquad (1)$$

Taking $\kappa_0 = 3.92$ W m^{-1}K^{-1}, the value measured for the single-domain film, and d equal to the DW periodicity (the mean ferroelectric domain size), the model provides an excellent fit to the experimental κ data (Figure 3b), giving $R_{DW} \approx (5.0 \pm 0.2) \times 10^{-9}$ Km^{2}W^{-1} (see Supp. Info. for deeper discussion). This value is similar to that calculated by Hopkins *et al.*[10] for BiFeO$_3$, and is also comparable to the effect of grain boundaries in, for instance, YSZ.[27] This result further supports the strong coupling between phonon transport and DWs in ferroelectric materials.

In parallel with the experimental measurements, phase-field simulations were performed to calculate the evolution of the ferroelectric domain patterns with strain [19,20] (Figure 3c). The results are in very good agreement with our experimental results (Figure 1 and 2) as well as the effect of the DWs on thermal conductivity[28] (see Supp. Info for details). Based on the fraction of DWs and domains for each domain pattern (Figure 3d),[19,20] the thermal conductivity of the films was then computed assuming that the κ of the domains is ten times higher than that of the DWs.[28] This

criterion was applied to all types of domains and DWs. Despite the simplicity of the model, the predicted thermal conductivity qualitatively reproduces the trend observed in the experiments (Figure 3a), namely, the local minimum around 0% epitaxial strain, coincident with a local maximum in the DW density, and the presence of a local maximum at small tensile strain and small compressive strain. As the tensile strain is increased, the DW density is predicted to continuously increase and, thus the thermal conductivity decreases, precisely as observed experimentally. On the compressive side, however, phase-field simulations predict a further reduction in κ as the DW density increases, which is not reflected in our experimental results on $PbTiO_3/SrTiO_3$. This is probably due to 180° DWs reducing the phonon propagation less than the 90° DWs.

In any event, both experiment and theory prove that the density of DWs is the main driving force in the modulation of κ in our $PbTiO_3$ thin films. The large thermal resistance of the 90° DWs is most probably due to the significant structural mismatch between the different types of domains (Figure 2h and Figure S12 in Supp. Info.). The 90° DWs involve a substantial change in the interatomic distances from one domain to another when crossing the DW (Figure 2h). A certain structural mismatch is also found across 180° DWs as Ti moves off center in opposite directions, but it is definitely smaller than 90° DWs. This may explain the slightly lower impact of the 180° DWs on the phonon transport. On the other hand, a polarization gradient occurs at all types of DWs, including the exclusively ferroelectric 180° DWs.[29] This gradient extends over several unit cells as shown in the atomic-scale STEM polarization maps (Figure 2g). These changes reflect the continuous variation in the off-centering displacement of the Ti cations as the DW is approached, making the region around it structurally inhomogeneous, which severely affects phonon transmission.

In summary, we have utilized epitaxial strain in single crystal thin films of ferroelectric $PbTiO_3$ to engineer a model system for investigating the effect of ferroelectric DWs on thermal conductivity. Our results demonstrate that DWs are very strong phonon scattering sites, and thus their distribution and density strongly affect the thermal transport in ferroelectrics. The design of ferroelectric patterns via strain engineering in epitaxially grown ferroelectric films allows tailoring κ in one single material, overcoming both the complexity involved in the fabrication of artificial multilayers systems and the random and uncontrolled distribution of grain boundaries in polycrystalline materials. In particular, a total reduction of κ by 61% with respect to the single-domain case is achieved in epitaxial $PbTiO_3$ films, the largest reduction at room temperature ever reported in ferroelectrics. This finding proves the suitability of ferroelectrics as active barriers to control thermal transport in phononic devices.

ASSOCIATED CONTENT

Supporting Information. Details of the experimental and theoretical methods employed in this work. Additional information related to the epitaxial growth of $PbTiO_3$ thin films and their structural characterization, the piezoresponse force microscopy experiments, the FDTR experimental set up, measurements, and analysis, and the details of the phase-field simulations.

This material is available free of charge via the Internet at http://pubs.acs.org.

Corresponding Author

*E-mail: eric.langenberg.perez@gmail.com

*E-mail: schlom@cornell.edumailto:eric.langenberg.perez@gmail.com

*E-mail: f.rivadulla@usc.edu

Author Contributions

E.L. and F.R. conceived the idea, and planned the research. D.G.S., J.M., N.D., and G.C. provided very useful insights throughout the project. E.L. grew the films, with the guidance of D.G.S and contributions of H.P. E.L. performed the PFM measurements and the data was analysed together with N.D. and G.C. D.S. characterized the thermal conductivity of the films by FDTR, with the feedback of J.M. D.B. and E.F. carried out additional thermal conductivity measurements and analysed the data together with F.R. M.E.H. prepared the samples for STEM, and analysed the results with D.A.M. E.L. performed the XRD characterization, including the RSMs. J.-J.W. and L.Q.C. realized the phase-field simulations. I.S. and S.G. have grown the rare-earth scandate substrate crystals by the Czochralski technique. E.L. and F.R. co-write the manuscript with the feedback from all of the other authors. All authors have given approval to the final version of the manuscript.

Notes

The authors declare no competing financial interest.

REFERENCES

(1)   Poudel, B.; Hao, Q.; Ma, Y.; Lan, Y.; Minnich, A.; Yu, B.; Yan, X.; Wang, D.; Muto, A.; Vashaee, D.; et al. High-Thermoelectric Performance of Nanostructured Bismuth Antimony Telluride Bulk Alloys. *Science (80-.).* **2008**, *320*, 634–638. https://doi.org/10.1126/science.1156446.

(2)   Costescu, R. M.; Cahill, D. G.; Fabreguette, F. H.; Sechrist, Z. A.; George, S. M. Ultra-Low Thermal Conductivity in W/Al2O3 Nanolaminates. *Science (80-.).* **2004**, *303*, 989–990.

(3)   Ravichandran, J.; Yadav, A. K.; Cheaito, R.; Rossen, P. B.; Soukiassian, A.; Suresha, S. J.; Duda, J. C.; Foley, B. M.; Lee, C. H.; Zhu, Y.; et al. Crossover from Incoherent to Coherent Phonon Scattering in Epitaxial Oxide Superlattices. *Nat. Mater.* **2014**, *13*, 168–172. https://doi.org/10.1038/nmat3826.

(4)   Böttner, H.; Chen, G.; Venkatasubramanian, R. Aspects of Thin-Film Superlattice Thermoelectric Materials, Devices, and Applications. *MRS Bull.* **2006**, *31*, 211–217. https://doi.org/10.1557/mrs2006.47.

(5)   Mante, A. J. H.; Volger, J. Phonon Transport in Barium Titanate. *Physica* **1971**, *52*, 577–604. https://doi.org/10.1016/0031-8914(71)90164-9.

(6)   Northrop, G. A.; Cotts, E. J.; Anderson, A. C.; Wolfe, J. P. Phonon Imaging of Highly Dislocated LiF. *Phys. Rev. Lett.* **1982**, *49*, 54–57. https://doi.org/10.1103/PhysRevLett.49.54.

(7)   Weilert, M. A.; Msall, M. E.; Wolfe, J. P.; Anderson, A. C. Mode Dependent Scattering of Phonons by Domain Walls in Ferroelectric KDP. *Z. Phys. B Condens. Matter* **1993**, *91*, 179–188. https://doi.org/10.1007/BF01315234.

(8)   Royo, M.; Escorihuela-Sayalero, C.; Íñiguez, J.; Rurali, R. Ferroelectric Domain Wall Phonon Polarizer. *Phys. Rev. Mater.* **2017**, *1*, 051402(R). https://doi.org/10.1103/PhysRevMaterials.1.051402.

(9)   Seijas-Bellido, J. A.; Escorihuela-Sayalero, C.; Royo, M.; Ljungberg, M. P.; Wojdeł, J. C.; Íñiguez, J.; Rurali, R. A Phononic Switch Based on Ferroelectric Domain Walls. *Phys. Rev. B* **2017**, *96*, 140101(R). https://doi.org/10.1103/PhysRevB.96.140101.

(10)   Hopkins, P. E.; Adamo, C.; Ye, L.; Huey, B. D.; Lee, S. R.; Schlom, D. G.; Ihlefeld, J. F. Effects of Coherent Ferroelastic Domain Walls on the Thermal Conductivity and Kapitza Conductance in Bismuth Ferrite. *Appl. Phys. Lett.* **2013**, *102*, 121903. https://doi.org/10.1063/1.4798497.

(11)   Ning, S.; Huberman, S. C.; Zhang, C.; Zhang, Z.; Chen, G.; Ross, C. A. Dependence of the Thermal Conductivity of $BiFeO_3$ Thin Films on Polarization and Structure. *Phys. Rev. Appl.* **2017**, *8*, 054049. https://doi.org/10.1103/PhysRevApplied.8.054049.

(12)   Ihlefeld, J. F.; Foley, B. M.; Scrymgeour, D. A.; Michael, J. R.; McKenzie, B. B.; Medlin, D. L.; Wallace, M.; Trolier-Mckinstry, S.; Hopkins, P. E. Room-Temperature Voltage Tunable Phonon Thermal Conductivity via Reconfigurable Interfaces in Ferroelectric Thin Films. *Nano Lett.* **2015**, *15*, 1791–1795. https://doi.org/10.1021/nl504505t.

(13)   Foley, B. M.; Wallace, M.; Gaskins, J. T.; Paisley, E. A.; Johnson-Wilke, R. L.; Kim, J. W.; Ryan, P. J.; Trolier-Mckinstry, S.; Hopkins, P. E.; Ihlefeld, J. F. Voltage-Controlled Bistable Thermal Conductivity in Suspended Ferroelectric Thin-Film Membranes. *ACS Appl. Mater. Interfaces* **2018**, *10*, 25493–25501. https://doi.org/10.1021/acsami.8b04169.

(14)   Liu, C.; Chen, Y.; Dames, C. Electric-Field-Controlled Thermal Switch in Ferroelectric Materials Using First-Principles Calculations and Domain-Wall Engineering. *Phys. Rev. Appl.* **2019**, *11*, 044002.

(15)   Maldovan, M. Sound and Heat Revolutions in Phononics. *Nature* **2013**, *503*, 209–217. https://doi.org/10.1038/nature12608.

(16)   Sklan, S. R. Splash, Pop, Sizzle: Information Processing with Phononic Computing. *AIP Adv.* **2015**, *5*, 053302. https://doi.org/10.1063/1.4919584.

(17)   Maire, J.; Anufriev, R.; Yanagisawa, R.; Ramiere, A.; Volz, S.; Nomura, M. Heat Conduction Tuning by Wave Nature of Phonons. *Sci. Adv.* **2017**, *3*, e1700027. https://doi.org/10.1126/sciadv.1700027.

(18)   Waser, R.; Pertsev, N. A.; Koukhar, V. G. Thermodynamic Theory of Epitaxial Ferroelectric Thin Films with Dense Domain Structures. *Phys. Rev. B - Condens. Matter Mater. Phys.* **2001**, *64*, 214103. https://doi.org/10.1103/PhysRevB.64.214103.

(19)   Li, Y. L.; Hu, S. Y.; Liu, Z. K.; Chen, L. Q. Effect of Substrate Constraint on the Stability and Evolution of Ferroelectric Domain Structures in Thin Films. *Acta Mater.* **2002**, *50*, 395–411. https://doi.org/10.1016/S1359-6454(01)00360-3.

(20)   Sheng, G.; Zhang, J. X.; Li, Y. L.; Choudhury, S.; Jia, Q. X.; Liu, Z. K.; Chen, L. Q. Domain Stability of $PbTiO_3$ Thin Films under Anisotropic Misfit Strains: Phase-Field Simulations. *J. Appl. Phys.* **2008**, *104*, 054105. https://doi.org/10.1063/1.2974093.

(21)   Damodaran, A. R.; Pandya, S.; Agar, J. C.; Cao, Y.; Vasudevan, R. K.; Xu, R.; Saremi, S.; Li, Q.; Kim, J.; McCarter, M. R.; et al. Three-State Ferroelastic Switching and Large Electromechanical Responses in PbTiO$_3$ Thin Films. *Adv. Mater.* **2017**, 1702069. https://doi.org/10.1002/adma.201702069.

(22)   Lichtensteiger, C.; Weymann, C.; Fernandez-Pena, S.; Paruch, P.; Triscone, J. M. Built-in Voltage in Thin Ferroelectric PbTiO$_3$ Films: The Effect of Electrostatic Boundary Conditions. *New J. Phys.* **2016**, *18*, 043030. https://doi.org/10.1088/1367-2630/18/4/043030.

(23)   Schmidt, A. J.; Cheaito, R.; Chiesa, M. A Frequency-Domain Thermoreflectance Method for the Characterization of Thermal Properties. *Rev. Sci. Instrum.* **2009**, *80*, 094901. https://doi.org/10.1063/1.3212673.

(24)   Malen, J. A.; Baheti, K.; Tong, T.; Zhao, Y.; Hudgings, J. A.; Majumdar, A. K. Optical Measurement of Thermal Conductivity Using Fiber Aligned Frequency Domain Thermoreflectance. *J. Heat Transfer* **2011**, *133*, 081601.

(25)   Roy, A. Estimates of the Thermal Conductivity and the Thermoelectric Properties of PbTiO$_3$ from First Principles. *Phys. Rev. B* **2016**, *93*, 100101(R). https://doi.org/10.1103/PhysRevB.93.100101.

(26)   Nan, C. W.; Birringer, R. Determining the Kapitza Resistance and the Thermal Conductivity of Polycrystals: A Simple Model. *Phys. Rev. B - Condens. Matter Mater. Phys.* **1998**, *57*, 8264. https://doi.org/10.1103/PhysRevB.57.8264.

(27)   Yang, H. S.; Bai, G. R.; Thompson, L. J.; Eastman, J. A. Interfacial Thermal Resistance in Nanocrystalline Yttria-Stabilized Zirconia. *Acta Mater.* **2002**, *50*, 2309–2317. https://doi.org/10.1016/S1359-6454(02)00057-5.

(28) Wang, J. J.; Wang, Y.; Ihlefeld, J. F.; Hopkins, P. E.; Chen, L. Q. Tunable Thermal Conductivity via Domain Structure Engineering in Ferroelectric Thin Films: A Phase-Field Simulation. *Acta Mater.* **2016**, *111*, 220–231. https://doi.org/10.1016/j.actamat.2016.03.069.

(29) De Luca, G.; Rossell, M. D.; Schaab, J.; Viart, N.; Fiebig, M.; Trassin, M. Domain Wall Architecture in Tetragonal Ferroelectric Thin Films. *Adv. Mater.* **2017**, *29*, 1605145. https://doi.org/10.1002/adma.201605145.